American Meteorological Society
11th Conf. on Mountain Meteorology
21-25 June 2004, Bartlett NH

8.2 PROCESSES LEADING TO INVERSION BUILDUP IN SMALL ENCLOSED BASINS

C. David Whiteman[1] and Thomas Haiden[2]

[1]Pacific Northwest National Laboratory, Richland, Washington
[2]Central Institute for Meteorology and Geodynamics, Vienna, Austria

1. INTRODUCTION

A meteorological field experiment was conducted from 17 October 2001 through 4 June 2002 on the Hetzkogel Plateau area 5 km south of Lunz, Austria in an area where a large number of limestone sinkholes or *dolines* of various sizes are found (Steinacker et al. 2002). As one part of the experiment, five sinkholes of various sizes were instrumented with temperature data loggers to determine what differences in temperatures would be found among the sinkholes and to investigate the effects of sinkhole geometry on the cooling. In this paper, we briefly summarize previous meteorological investigations in basins, describe our experiments and observational findings, and develop an analytical model to explain the observations. The model suggests that the differences in cooling between sinkholes is not due to different drainage areas or sinkhole volumes, but can be explained by differences in the surface energy budgets at the sinkhole floors. Especially important in the cooling is the sky-view factor, the fraction of the sky hemisphere that is visible from the sinkhole floor.

2. BACKGROUND

Basin inversions have been studied previously in Slovenia (Petkovsek and Rakovec 1983; Vrhovec 1991; Rakovec et al. 2002), Japan (Magono et al. 1982; Maki and Harimaya 1988; Maki et al. 1986; Kondo et al. 1989; Yoshino 1984; Iijima and Shinoda 2000), the western US (Whiteman et al. 1996; Clements et al. 2003) and in the limestone ranges of the European Alps (Geiger 1965). Most of the basins studied to date have been major basins containing population centers, where high industrial emissions and persistent inversions cause air pollution problems.

Most studies of basin inversions have emphasized the role of downslope flow convergence in the formation of valley and basin inversions and the continued cooling that occurs in the valley and basin atmospheres during nighttime. Other investigators (Thompson 1986; Clements et al. 2002), however, have noted the development of basin temperature inversions and the continuous cooling of the basin atmosphere in situations where downslope flows could not be detected on the sidewalls or when downslope flows weakened significantly during the night. In these situations, the cooling cannot be caused solely by convergence of downslope flows, the explanation most commonly offered for nighttime cooling and inversion buildup in valleys and basins. Alternative hypotheses are available to explain the continued cooling. For example, inversions and nighttime cooling clearly occur over flat, homogeneous terrain where downslope flows are not present. In these situations, the surface energy budget plays an important role and heat is lost through turbulent sensible and radiation flux divergences, processes that are driven by the net loss of longwave radiation from the surface.

The small closed basins on the Hetzkogel Plateau have been previously studied by other investigators, following the reports of extreme minimum temperatures in the largest doline, the Gruenloch Basin (Aigner 1952; Schmidt 1930, 1933). Following this early work, two tethered balloon sounding campaigns were conducted in the Gruenloch in 1953 and 1954 (Sauberer and Dirmhirn 1954, 1956). The first of these tethered balloon campaigns, conducted in March with wintertime snow cover, found air temperatures as low as -30.5°C on the basin floor and the development of an impressive 20°C inversion over a depth of 70 m. An unpublished dissertation by Litschauer (1962) investigated many scientific questions on basin climatology in Austria and in the Gruenloch in particular, comparing temperature minima and considering the effects of basin size and shape. In the present paper, we use temperature data from the floors of five dolines in the Gruenloch region, comparing the cooling observed in the sinkholes of different size and shape.

3. METHODOLOGY

A topographic contour map of a part of the Hetzkogel Plateau is shown in Fig. 1, indicating the individual dolines D0 through D4 and the measurement sites. Figure 2 shows topographic cross sections through the sinkholes, while Table 1 summarizes the dolines' geometrical characteristics.

The temperature data were collected using Hobo H8 Pro temperature data loggers (Onset Computer, Inc., Bourne, Massachusetts). The specifications and operating characteristics of these loggers have been reported by Whiteman et al. (2000). The data logger thermistors were exposed in radiation shields 1.4 m above the ground on the sinkhole floors, with data sampled at 5-min intervals. Supplementary measurements were made with three automatic weather stations noted in Fig. 1 by their site designators, GL, LS, and HK. The temperature loggers were operated from 17 October 2001 through 4 June 2002. Because the dolines are located on the same plateau the synoptic conditions are the same for all dolines.

Corresponding author address: C. David Whiteman, PNNL, P. O. Box 999, Richland, WA 99352

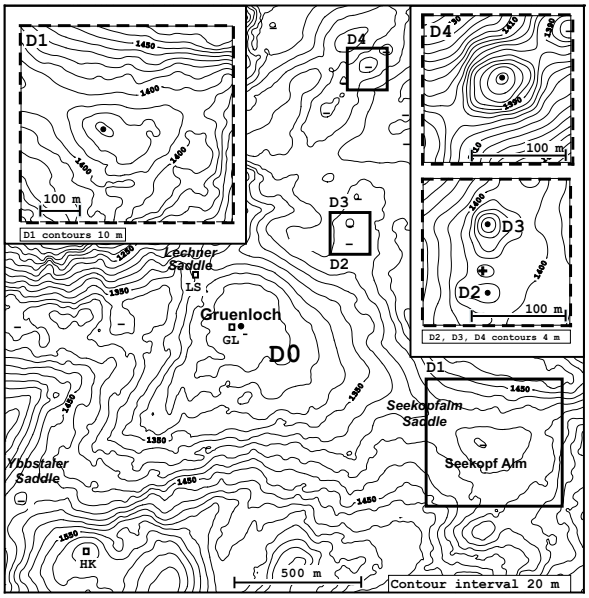

Fig. 1. Topographic map of the Gruenloch doline (D0) and its surroundings showing the locations of selected temperature data loggers at the doline floors (filled circles), and automatic weather stations (squares). Detailed topographic maps for the areas surrounding dolines D1, D2 and D3, and D4 (solid rectangles) are shown as inset figures (dashed rectangles). Note the different length scales and contour intervals in the inset figures. Negative signs on the main map identify the centers of dolines.

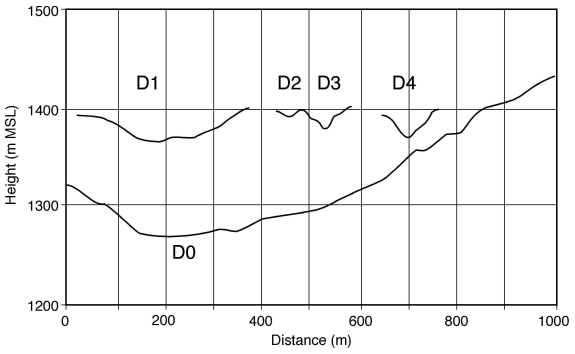

Fig. 2. Topographic cross sections through the five dolines. The origin of the D0 cross section starts at the Lechner Saddle. The other cross sections are plotted at arbitrary distances on the x-axis, but at actual heights on the y-axis. The sections are made on lines connecting the doline floors to the lowest saddles.

4. OBSERVATIONS

Time series of measured air temperatures at the floors of the five dolines on the clear, undisturbed night of 18-19 October 2002 are shown in Fig. 3. The floors experience their maximum temperatures in the early afternoon and their minimum temperatures near sunrise (astronomical sunset = 1702 Central European Standard Time (CEST); astronomical sunrise = 0628 CEST). The coldest temperatures occur at the floors of D0 and D1. The warmest temperatures occur at D2. Surprisingly, the temperature traces are nearly identical from mid-afternoon until sunrise for D0 and D1, dolines whose drainage areas differ by a factor of 8.6. Similarly, D3 and D4 also have nearly identical nighttime temperature courses. The near-equality of temperatures at dolines D0 and D1 are illustrated further in Fig. 3, which shows that the temperatures differences between the two sinkholes are generally less than 1℃ from mid-afternoon through sunrise on clear days and nights. This does not vary with season, and is valid also on days with snow cover (e.g., December 2-3). Further, the days illustrated in Fig. 3 had different day-night temperature ranges. The 1500 CEST to sunrise temperature drops were 16.9, 23.9, 12.8, 12.9 and 7.4℃ on May 30, Oct 18, Nov 3, Nov 11 and Dec 2, respectively. Temperatures at the shallow, higher elevation sinkhole D1 are sometimes subject to wind intrusions. When these intrusions occur, temperatures warm abruptly. After the intrusion ends, temperatures again become matched between the two sinkholes.

The near-equality of surface temperatures in the two sinkholes is an interesting and counterintuitive result. The usual preconception is that temperatures fall in sinkholes because cold air drains into the basin from the surrounding drainage area, suggesting that the cooling will be a function of drainage area and the

Table 1. Topographic characteristics of the five dolines. Sky-view factors as given by Litschauer (1962) for D0, D2-D4, and from a direct measurement for D1. Total drainage areas for D2 and D3 are, to a good approximation, identical.

Basin	D0	D1	D2	D3	D4
elevation of doline floor (m MSL)	1270	1368	1393	1381	1372
outflow depth h (m)	54	26	7	19	22
diameter at h (m)	600	250	45	75	76
drainage area A below h (10^3 m^2)	295	51	1.6	4.44	4.56
volume V below h (10^3 m^3)	7,000	550	2.7	19.3	41
total drainage area A_T (10^3 m^2)	2,120	245	313	313	334.5
sky-view factor f_v	0.91	0.88	~0.6	~0.6	~0.6

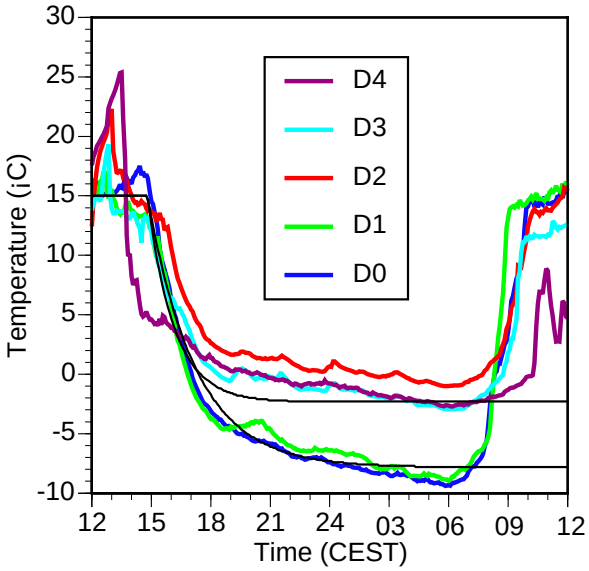

Figure 3. Observed temperatures on 18-19 October 2001 in sinkholes D0-D4 (colored lines, see legend). Also shown (black lines) are simulations for sky-view factors of 0.9 (lower curve), and 0.6 (upper curve).

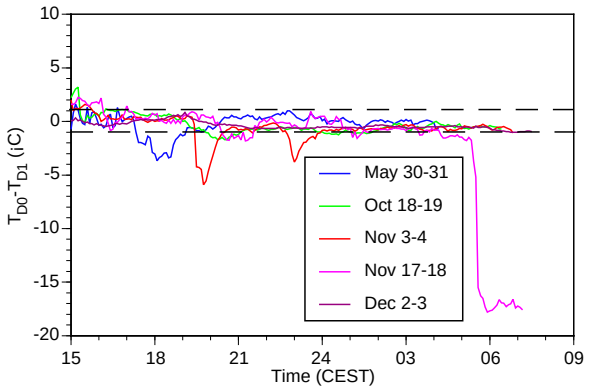

Fig. 4. Time series of temperature differences between the floors of dolines D0 and D1 on selected dates in 2001-2002. Data are plotted from 1500 CEST until sunrise. Dashed lines indicate the ± 1℃ boundaries.

volume of the enclosed basin. The drainage would allow the enclosed volume to receive the benefit of near-surface air that is cooled over the entire drainage area. In fact, the drainage areas, volumes and other geometrical characteristics of basins D0-D4 as given in all but the last row of Table 2 appear to be unrelated to the nighttime temperatures attained on the basin floors. Our investigations of other potential measures of cooling (e.g., temperature falls, inversion strengths, inversion depths, total heat loss to various heights) come to this same result. An alternative hypothesis is that the cooling in the range of sinkhole sizes investigated are driven by the surface energy budgets at the sinkhole floors rather than by drainage flows. These energy budgets should depend critically on the fraction of the sky hemisphere that is visible from the sinkhole center (the *sky-view factor*) because low sky-view factors reduce the heat loss from the basin because of enhanced back-radiation from the relatively warm (relative to the sky radiation) sidewalls that enclose the basin. This hypothesis is suggested by the last row of Table 2, in which the sky-view factors have roughly the same ordering as the sinkhole temperature minima.

5. ANALYTICAL MODEL

The fact that the sinkholes D0 and D1, despite their different sizes, depths, and drainage areas experience very similar nighttime temperatures is a significant finding that forces us to revisit the theory of nighttime cooling in closed basins. Whereas temperatures at D0 and D1 differ markedly during daytime (due to different local sunrise and sunset times, different degrees of inversion breakup, etc.) they approach each other soon after local sunset and remain within ~1℃ throughout the night. Any head start of D1 compared to D0 in terms of cooling is rapidly lost early in the night. The short time constant of the process suggests the presence of a strong negative feedback of temperature on the cooling process. This is confirmed by the behavior of the temperature curves after other intermittent disturbances (Fig. 4). D1, which is more susceptible to the ambient wind, manages to catch up quickly with the temperature trace at D0 after such episodes.

Let us consider limiting cases. The temperature at the bottom of a sinkhole could be the result of a cooling process that is (almost) independent of temperature. Then intermittent warming episodes would not be energetically 'forgotten', leading to a permanent cooling lag in the system. In the other extreme, the temperature could be the result of a quasi-equilibrium between cooling and (almost) equal opposing warming processes, where any temperature change initiates strong counteracting mechanisms. In such a system the temperature would quickly recover once ambient wind effects cease. Observational evidence suggests that during most of the night the air near the bottom of the sinkhole is rather close to the strong feedback, quasi-equilibrium state. Below, we present a highly simplified model of near-surface cooling to analyze this quasi-equilibrium theoretically.

Over flat terrain under undisturbed conditions with weak synoptic flow nighttime cooling of near-surface air is primarily caused by net longwave radiative loss from the uppermost soil layer (and vegetation, if present). Radiative cooling of the soil at the soil-air interface produces a downward sensible heat flux from the adjacent air which acts as a negative feedback to counteract the cooling of the soil. Once the uppermost soil layer has cooled sufficiently, an upward sensible heat flux from warmer, deeper layers will begin to counteract surface cooling as well. A third negative feedback is associated with the longwave radiative flux itself. The more the surface cools relative to the air at higher levels, the smaller the net outgoing radiation will be. As a result of the negative feedbacks, near-surface

temperature decreases more and more slowly during the course of a night.

In what way is the cooling process in a closed basin different from the process over flat terrain? The concave shape of the topography keeps the air close to the basin floor from being mixed by the ambient flow once a stable stratification has developed. Thus at the basin floor windless conditions will be established earlier in the night, and maintained more easily against any shear-induced turbulence which may be intermittently generated at higher levels even in weak flow situations. Once the temperature near the basin floor has become several degrees colder than the air at the basin rim there will be very little direct advection of air from the rim all the way down to the basin floor. By cooling down fastest (because it does not move), the air at the basin floor quickly isolates itself from air at higher levels. Thus, while katabatic flows may still drain towards the basin they do not directly lead to air exchange near the basin floor but enter the basin atmosphere at higher levels. The lack of mass exchange between the sinkhole floor and the slopes could explain why D0 and D1, despite their different topographic characteristics, show extremely similar temperature traces even during the initial, rapid cooling phase.

Another consequence of concave topography is the reduced view of the sky. It means that part of the downward longwave radiation at the basin floor does not originate in the atmosphere but from surrounding terrain. This can be expressed in the form of a sky-view factor $f_V = \cos^2 \alpha$, where α is the average elevation angle of the horizon (Marks and Dozier 1979). The downward longwave radiation flux density assumes the form

$$L^{\downarrow} = f_V \varepsilon_A \sigma T_A^4 + (1 - f_V) \varepsilon_S \sigma T_S^4 , \qquad (1)$$

where ε denotes emissivity, σ is the Stefan-Boltzmann constant, and the subscripts *A* and *S* denote the atmosphere and surface, respectively. Table 1 shows that the two coldest dolines D0 and D1 have sky-view factors close to 0.9, whereas the smaller dolines are estimated to have values around 0.6. In all cases the effect of forest surrounding the basins was taken into account in the determination of the sky-view factor (Litschauer 1962).

Eq. (1) is strictly valid only if the surface temperature T_S is uniform. In the case of basin cooling we must take into account that the basin wall temperature T_W will be different from, and on average warmer than, the basin floor surface temperature T_S. This leads to a stronger increase of incoming radiation than predicted by (1). Within the framework of simple analytical modeling, an improved estimation of reduced sky-view effects can be derived as follows. The upward longwave flux is given by

$$L^{\uparrow} = \varepsilon_S \sigma T_S^4 , \qquad (2)$$

as over flat terrain. The downward longwave flux at the basin floor consists of a contribution from the atmosphere and a contribution from the basin sidewalls.

$$L^{\downarrow} = f_V \sigma \varepsilon_A T_A^4 + (1 - f_V) \sigma \varepsilon_S T_W^4 . \qquad (3)$$

where the sidewall temperature T_W will be somewhere in between the basin floor temperature T_S and the rim temperature T_A. This can be expressed in the form $T_W = (1-g)T_S + g T_A$, where g is a parameter that depends on the geometry of the basin. Combining (2), (3), and the expression for T_W gives for the net outgoing longwave radiation

$$L_{NET} = L^{\uparrow} - L^{\downarrow} = f_V \sigma (\varepsilon_S T_S^4 - \varepsilon_A T_A^4) + g(1 - f_V) \sigma \varepsilon_S (T_S^4 - T_A^4) \qquad (4)$$

The second term on the r.h.s. of (4) is zero if the sidewall temperature is identical to the floor temperature (g = 0). In this case Eq. (4) reduces to the standard expression presented in the literature (Marks and Dozier 1979).

Under windless conditions the sensible heat flux from the atmosphere to the ground will be small (Clements et al. 2003), ultimately approaching the molecular flux value. Thus downward longwave radiation and upward sensible heat flux from deeper soil layers remain the only processes counteracting longwave cooling of the soil surface. This is illustrated schematically in Figure 5 where a surface soil layer with thickness δ loses heat by longwave emission, and receives heat from two reservoirs at constant, or slowly varying, temperatures T_A and T_D.

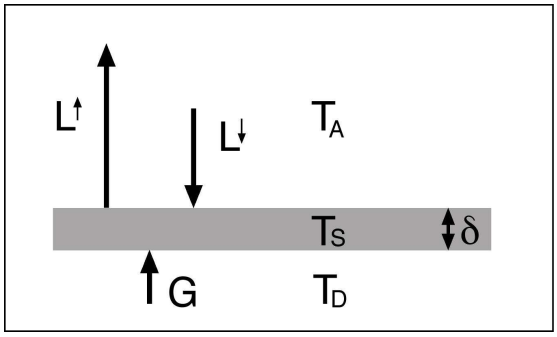

Figure 5. Idealized three-layer model of surface cooling corresponding to Eq. (4). The surface soil layer at a temperature T_S loses heat by longwave radiation exchange with the atmosphere at an effective radiation temperature T_A, and gains heat by conduction from a deeper soil layer at a temperature T_D.

A simplified prognostic equation for the time evolution of soil surface temperature can be written in the form

$$\delta c_S \rho_S \frac{dT_S}{dt} = -L_{NET} + G = f_V \sigma(\varepsilon_A T_A^4 - \varepsilon_S T_S^4) + g(1-f_V)\sigma\varepsilon_S (T_A^4 - T_S^4) + \frac{\nu_S}{D}(T_D - T_S), \quad (5)$$

where c_S, ν_S, and ρ_S are the specific heat capacity, thermal conductivity, and density of the surface soil layer. The length scale *D* represents the effective depth over which the temperature difference $T_D - T_S$ extends. Eq. (5) is highly idealized since it reduces the heat exchange at the interface of two continuous media to a three-layer problem. Models employing this type of formulation for the soil heat flux are also known as 'force-restore' models. They have been used in global circulation modeling (see e.g. Bhumralkar 1975) and boundary layer modeling (Stull 1988) and represent an approximation to the vertical diffusion equation equivalent to considering only the leading sinusoidal mode of the forcing (Dickinson 1988). For our problem, the approach provides the simplest possible way of representing the cooling process with the feedbacks envisaged above. If we define as an initial condition $T_S(t=0) = T_{S0}$, and linearize (5) by replacing T_S^4 with $T_{S0}^4 + 4T_{S0}^3(T_S - T_{S0})$, we obtain after some re-ordering of terms the equation

$$\delta c_S \rho_S \frac{dT_S}{dt} = AT_A^4 + 3BT_{S0}^4 + \frac{\nu_S}{D}T_D - (4\,B\,T_{S0}^3 + \frac{\nu_S}{D})T_S, \quad (6)$$

where

$A = f_V \sigma \varepsilon_A - g(1-f_V)\sigma\varepsilon_S$, and

$B = f_V \sigma \varepsilon_S - g(1-f_V)\sigma\varepsilon_S$.

Eq. (6) is of the form $dT_S/dt = a - bT_S$, giving a negative-exponential solution for the soil surface temperature as a function of time

$$T_S(t) = T_{S0}e^{-t/\tau} + T_{S\infty}(1 - e^{-t/\tau}), \quad (7)$$

where

$$\tau = \frac{\delta c_S \rho_S}{4BT_{S0}^3 + \frac{\nu_S}{D}}, \text{ and}$$

$$T_{S\infty} = \frac{AT_A^4 + 3BT_{S0}^4 + \frac{\nu_S}{D}T_D}{4BT_{S0}^3 + \frac{\nu_S}{D}}.$$

The temperature in the surface soil layer asymptotically approaches the equilibrium temperature $T_{S\infty}$, which is a function of the temperatures of the two reservoirs. Once the temperature gets close to the equilibrium value, net longwave radiation is nearly balanced by the ground heat flux, and further cooling of the surface is small. The time constant of the approach is largely determined by, and rather sensitive to, soil parameters.

Using the parameter values listed in Table 2, we have evaluated (7) for the sky-view factors 0.9 and 0.6 corresponding to sinkholes D0-D1 and D2-D4, respectively. The reservoir temperatures were set equal to the temperature of the surface at the beginning of the cooling process. Atmospheric emissivity was set to a typical value of 0.7 (Holtslag and de Bruin 1988). The resulting net outgoing longwave flux assumed realistic values of about 80 W m^{-2} at the beginning, and strongly decreased to values on the order of 10-20 W m^{-2} later in the night. A rather small thickness of the order of 2 cm (cf. Table 2) has to be assumed for the thermally active surface soil layer to obtain the rapid temperature drop during the first hours of the cooling. The sidewall temperature parameter had to be set to *g* = 0.8, corresponding to sidewalls significantly closer to basin rim than basin floor temperature. Figure 3 shows a comparison of modeled surface temperature (thin black lines) and observed temperatures at 1.5 m height. We assume that even during calm conditions the temperature at 1.5 m height evolves largely parallel to the surface temperature. The model reproduces the basic characteristics of the observed cooling curves, in particular their dependence on the sky-view factor. This suggests that the sky-view factor is indeed the most important topographic parameter controlling basin cooling. Additional evidence for this hypothesis is provided by Litschauer (1962), who noted that the 'Untere Legsteinalm' sinkhole (not studied here) reportedly experiences temperatures almost as low as the Gruenloch (D0) even though it has a much lower saddle. Its sky-view factor is 0.88 (Litschauer 1962) and is thus very similar to D0 and D1.

The dominant influence of the sky-view factor or aspect ratio on the cooling, and the near-independence from other topographic parameters such as absolute size and depth obviously cannot carry over to ever smaller basins. We do not observe inversions as strong as those reported here (20-30 K) in depressions of, say, 1 m depth. As the basin gets shallower, complete protection from shear-induced turbulence will no longer occur. But even in cases where ambient winds were so weak that a completely calm state could be attained, vertical temperature gradients would be limited by direct radiative heat exchange within the air. Furthermore, only in a sufficiently deep basin can cooling of the bulk of the basin atmosphere lead to a significant reduction of downward longwave radiation at the basin floor. During the course of the night the surface at the floor of a deep sinkhole radiatively 'sees' an increasingly colder atmosphere. This could explain why the observed temperature curves in Figure 3 do not approach a constant equilibrium temperature as in the idealized

Table 2. Parameter values used to compute the idealized cooling curves shown in Figure 3. Soil parameters and atmospheric emissivity were chosen following Pielke (1984) and Holtslag and de Bruin (1988), respectively.

Param.	Value	Comment
T_A=T_{S0}	288.15 K	corresponding to observed temperature at the beginning of cooling
T_D	278.15 K	tuned to approx. match equilibrium temperature T_∞
ε_A	0.7	typical clear-sky atmospheric emissivity
ε_S	0.95	average for mixture of grass and limestone gravel
δ	0.02 m	tuned to match rapid initial cooling
D	0.5 m	typical penetration depth of surface cooling
ρ_S	1500 kg m^{-3}	average for mixture of light soil and rock
c_S	1000 J kg^{-1} K^{-1}	
ν_S	1 W m^{-1} K^{-1}	

model, but keep dropping at a low rate throughout the night. The slow cooling during the second half of the night would then merely be the result of slowly decreasing T_A. Observational evidence for this hypothesis has been presented by Eisenbach et al. (2003). Their Figure 2 shows that during the second half of the night the temperatures at the basin floor and at the height of the lowest saddle (50 m above the floor) decrease at the same rate. This 'basin atmosphere' effect would be weak or absent in very shallow basins.

The expression derived for the equilibrium temperature can be used to explain observations of extreme sinkhole temperature minima and intense inversion buildup that occur after fresh snowfalls. Record temperature minima in sinkholes and basins generally occur on clear, windless nights following a fresh fall of new snow (Geiger 1965). The snow cover provides an insulating layer that reduces the upward ground heat flux that normally counters long-wave radiation loss from the surface. The outgoing longwave flux from a fresh snow surface, in contrast, differs little from that of soil at the same temperature, since the emissivities are comparable. With smaller thermal conductivity, the equilibrium temperature in a shallow layer at the upper surface of the snowpack is thus reduced from the case with no snow cover.

6. CONCLUSIONS

The observed close correspondence of basin floor cooling in two sinkholes of different size but with similar aspect ratio appeared to be unrelated to the sinkhole drainage areas or volumes, suggesting that other processes besides cold air drainage are responsible for the cooling observed during clear sky conditions. An idealized three-layer surface energy budget model, in which we have extended the sky-view factor concept to account for radiation from sidewalls that have a temperature intermediate between the basin floor and the above-basin atmosphere, is used to test whether the surface energy budgets at the sinkhole floors can explain the observed cooling among the five sinkholes. The surface energy budget model, while not including advection, is able to account for the temperature differences among the sinkholes. The model shows that the cooling is strongly dependent on the sky-view factors at the sinkhole floors. Sinkholes that see little of the sky receive large back-radiation from the surrounding and relatively warm sidewalls and, so, do not cool as strongly as sinkholes that have more open views of the sky. After a rapid initial cooling phase, a near-equilibrium is established between net longwave radiative loss at the surface and the upward flux of heat from the ground. The model also provides a physical explanation for the extreme temperature minima that occur on clear, windless nights following a fresh fall of snow. Further information on this research can be found in an upcoming journal paper (Whiteman et al. 2004).

Acknowledgements

We thank the other participants of the 2001-2002 Gruenloch experiments. One of the authors (CDW) wishes to acknowledge research support from the U.S. Department of Energy's (DOE) Vertical Transport and Mixing (VTMX) program under the auspices of the Environmental Meteorology Program of the Office of Biological and Environmental Research. His contributions were made at PNNL, which is operated for DOE by Battelle Memorial Institute.

REFERENCES

Aigner, S., 1952: Die Temperaturminima im Gstettnerboden bei Lunz am See, Niederösterreich [The minimum temperatures in the Gstettner basin near Lunz, Lower Austria]. *Wetter und Leben, Sonderheft*, 34-37.

Bhumralkar, C. M., 1975: Numerical experiments on the computation of ground surface temperature in an atmospheric general circulation model. *J. Appl. Meteor.*, **14**, 1246-1258.

Clements, C. B., C. D. Whiteman, and J. D. Horel, 2003: Cold air pool structure and evolution in a mountain basin: Peter Sinks, Utah. *J. Appl. Meteor.*, **42**, 752-768.

Dickinson, R. E., 1988: The force-restore model for surface temperatures and its generalization. *J. Climate*, **1,** 1086-1097.

Eisenbach, S., B. Pospichal, C. D. Whiteman, R. Steinacker, and M. Dorninger, 2003: Classification of cold air pool events in the Gstettneralm, a sinkhole in the Eastern Alps. *Extended Abstracts, Int. Conf. Alpine Meteorology and MAP-Meeting*,

MeteoSwiss Publication no. 66, 157-160. [Available from MeteoSwiss, Zurich, Switzerland]

Geiger, R., 1965: *The Climate near the Ground*. Cambridge: Harvard University Press. 482 pp.

Holtslag, A. A. M., and H. A. R. de Bruin, 1988: Applied modeling of the nighttime surface energy balance over land. *J. Appl. Meteor.,* **27,** 689-704.

Iijima, Y., and M. Shinoda, 2000: Seasonal changes in the cold-air pool formation in a subalpine hollow, central Japan. *Int. J. Climatol.*, **20**, 1471-1483.

Kondo, J., T. Kuwagata, and S. Haginoya, 1989: Heat budget analysis of nocturnal cooling and daytime heating in a basin. *J. Atmos. Sci.*, **19**, 2917-2933.

Litschauer, D., 1962: Untersuchung der Entwicklung von Kaltluftseen in Dolinen- und Beckenlagen [Investigation of the development of cool air pools in sinkholes and basins]. Dissertation, University of Vienna, 129pp.

Magono, C., C. Nakamura, and Y. Yoshida, 1982: Nocturnal cooling of the Moshiri Basin, Hokkaido in midwinter. *J. Meteor. Soc. Japan*, **60**, 1106-1116.

Maki, M., and T. Harimaya, 1988: The effect of advection and accumulation of downslope cold air on nocturnal cooling in basins. *J. Meteor. Soc. Japan*, **66**, 581-597.

_____, T. Harimaya, and K. Kikuchi, 1986: Heat budget studies on nocturnal cooling in a basin. *J. Meteor. Soc. Japan*, **64**, 727-740.

Marks, D., and J. Dozier, 1979: A clear-sky longwave radiation model for remote alpine areas. *Arch. Met. Geoph. Biokl.,* **B27**, 159-187.

Petkovsek, Z., and J. Rakovec, 1983: Modelling of cool pool dissipation. *Razprave Papers,* Ljubljana, Letnik **27** (2), 53-63.

Pielke, R. A., 1984: *Mesoscale Meteorological Modelling*. Academic Press, San Diego, 612p.

Rakovec, J., J. Merse, S. Jernej, and B. Paradiz, 2002: Turbulent dissipation of the cold-air pool in a basin: Comparison of observed and simulated development. *Meteorol. Atmos. Phys.*, **79**, 195-213.

Sauberer, F., and I. Dirmhirn, 1954: Über die Entstehung der extremen Temperaturminima in der Doline Gstettner-Alm. [On the occurrence of extreme temperature minimums in the Gstettner-Alm Doline]. *Arch. Meteor. Geophys. Bioclimatol.*, *Ser. B*, **5**, 307-326.

_____, and I. Dirmhirn, 1956: Weitere Untersuchungen über die kaltluftansammungen in der Doline Gstettner-Alm bei Lunz im Niederösterreich. [Further investigations of the cold air buildup in the Gstettner-Alm doline near Lunz in lower Austria]. *Wetter Leben,* **8**, 187-196.

Schmidt, W., 1930: Die tiefsten Minimumtemperaturen in Mitteleuropa [The lowest minimum temperatures in central Europe]. *Die Naturwissenschaften*, **18**, 367-369.

_____, 1933: Kleinklimatische Beobachtungen in Österreich [Microclimatic observations in Austria]. *Geographischer Jahresbericht aus Österreich*, **XVI**, *Separatabdruck*, 53-59.

Steinacker, R., M. Dorninger, S. Eisenbach, A. M. Holzer, B. Pospichal, C. D. Whiteman, and E. Mursch-Radlgruber, 2002: A sinkhole field experiment in the Eastern Alps. Preprints, 10th Conf. on Mountain Meteorology, 17-21 June 2002, Park City, UT. Amer. Meteor. Soc., Boston, MA, 91-92.

Stull, R. B., 1988: *An Introduction to Boundary Layer Meteorology.* Kluwer, Dordrecht, 670pp.

Thompson, B. W., 1986: Small-scale katabatics and cold hollows. *Weather*, 41, 146-153.

Vrhovec, T., 1991: A cold air lake formation in a basin - a simulation with a mesoscale numerical model. *Meteor. Atmos. Phys.,* **46**, 91-99.

Whiteman, C. D., T. Haiden, B. Pospichal, S. Eisenbach, and R. Steinacker, 2004: Minimum temperatures, diurnal temperature ranges and temperature inversions in limestone sinkholes of different size and shape. *J. Appl. Meteor.* In press.

_____, J. M. Hubbe, and W. J. Shaw, 2000: Evaluation of an inexpensive temperature data logger for meteorological applications. *J. Atmos. Oceanic Technol.*, **17**, 77-81.

_____, T. B. McKee, and J. C. Doran, 1996: Boundary layer evolution within a canyonland basin. Part I. Mass, heat, and moisture budgets from observations. *J. Appl. Meteor.*, **35**, 2145-2161.

Yoshino, M. M., 1984: Thermal belt and cold air drainage on the mountain slope and cold air lake in the basin at quiet, clear night. *Geo Journal*, **8.3**, 235-250.